

CLICHE - A GENERALLY APPLICABLE AND PRACTICABLE OFFSHORE EXPLOSION MODEL

C.A. Catlin\*

This paper presents the theory and application of the British Gas Confined Linked Chamber Explosion model CLICHE. The modelling assumptions are described which enable CLICHE to yield predictions in practicable computing times. CLICHE predictions of explosions both in empty confined volumes and of turbulent flame acceleration through concentric rings of obstacles are compared with field-scale experimental data of British Gas and TNO. Its application to offshore explosions is demonstrated by comparing predictions against British Gas experimental data on representative offshore modules and also against numerical predictions of the Chr. Michelsen Institute FLACS code as presented to the Piper Alpha inquiry.

INTRODUCTION

In studying the scenarios which could have led to the explosion on Piper Alpha, the inquiry emphasised the complexity of the problem of making explosion hazard assessments of offshore platforms. One of the primary contributory factors is the complexity of the explosion process itself, the understanding of which is presently far from complete. Currently, there is no simply applied method for assessing the consequences of explosion scenarios, which is both sufficiently versatile to cater for the many parameters that influence explosion behaviour, and which can also provide high confidence in the prediction. Even when only considering an explosion in one module, it is still necessary to evaluate a variety of scenarios for differing releases of flammable material and potential ignition sources. The number of cases that need to be considered grows when the hazard assessment is extended to the whole platform, and further when structural changes are considered as ways of lessening the explosion consequences. One of the most taxing problems at present is to find a way of ensuring that unacceptable explosion hazards are excluded during the design of new platforms. Thus, an easily used predictive technique could potentially provide an additional design tool.

There are many contributory factors to the present incomplete understanding of explosion behaviour. A primary problem is obtaining sufficient experimental data, since there are so many parameters to be studied. Flame acceleration is known to be sensitive to the orientation of obstacles; their relative positions to venting routes; perimeter confinement; obstacle sizes and separation; initial turbulence; fuel type and fuel/air ratio (Chamberlain (1), Harris and Wickens (2)). Reduced scale experimental studies provide the only practicable source of data. However, these data

\* British Gas Research and Technology Division, Midlands Research Station.

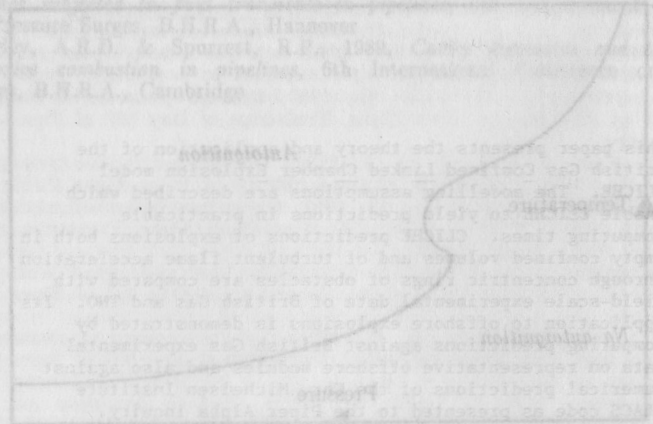


FIGURE 1 Schematic pressure-temperature history for explosion

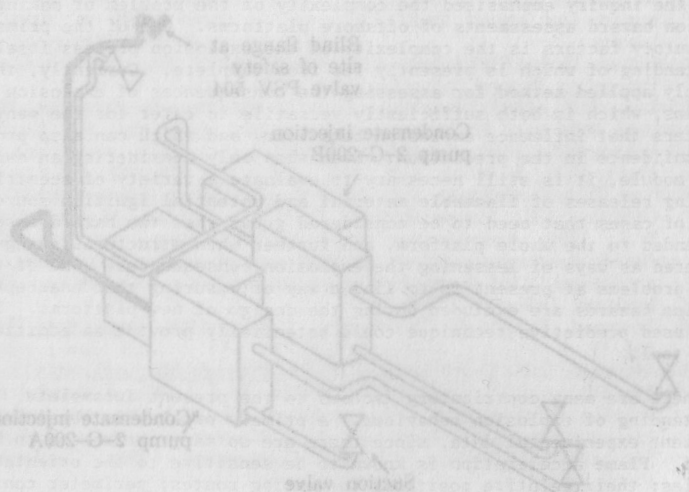


FIGURE 2 General arrangement of condensate injection pumps and associated lines on Piper Alpha, shaded line is one in which possibility of autoignition was examined

are not necessarily representative of full-scale explosion behaviour since the flame speeds and overpressures are typically larger at full-scale. Empirically based scaling relationships exist for low flame speeds in certain geometries (Van Wingerden (3)) but in general there is not a simple relationship between the two scales (Catlin and Johnson (4)). This has prompted a number of studies into methods for compensating for scale-effects in reduced scale experiments (Taylor (5), Catlin (6), (3), (4)) but these methods are as yet of uncertain predictive accuracy (British Gas (7)).

The limitations in experimental modelling, compounded by the need to interpret the wide range of explosion behaviour observed in experiments, has resulted in the development of mathematically based predictive techniques. There are a variety of different types (7) varying from empirically based models (VENTEX) (1) to the fundamentally based numerical models (FLACS) which solve the governing partial differential equations (Bakke (8)). The simpler models have the advantage that they provide answers on small computers in very short run times and the corresponding disadvantage that they embody many approximations, thus limiting their applicability. Being empirically based, they are also limited by the lack of relevant full-scale data. The large numerical models on the other hand, which are capable of predicting the detailed fluid dynamics and flame movement, require considerable run times, even on powerful parallel computers, making them expensive and time consuming when conducting a general survey.

The above observations led British Gas to embark upon the development of the CLICHE model to provide a practicable means of performing offshore explosion hazard assessments. The aim is to make the model as fundamentally based as possible, with the capability of being applied to single or multiple modules incorporating any layout of plant.

CLICHE (Confined Linked Chamber Explosion) was originally developed to study confined explosions in buildings involving flame propagation from one room to another. The basic modelling assumptions used in CLICHE are well established (Fairweather and Vasey (9), Chippett (10)) in applications to confined explosions in a single empty vessel which has a large fraction of its perimeter area closed. Typically these chambers have a single vent to atmosphere. CLICHE is a generalisation of this concept to a sequence of interlinked explosion chambers. Whilst there are parts of offshore platforms which are comparatively empty, with all round confinement, other parts, typically the process areas, include large amounts of pipework, plant and process vessels. The drag induced by such obstacles in the flow ahead of a flame causes a pressure gradient. Such regions are therefore represented in CLICHE by a sequence of chambers and the pressure gradients modelled by applying appropriate resistance terms at inter-chamber vents.

The parameters that are required to model drag and the interaction between the flame and the obstacles are determined from an accurate geometric description of the layout of plant within a module, which is stored in a numerical database accessed by CLICHE. A fundamentally based combustion sub-model is used to determine both laminar and turbulent burning velocities, the predictions of which have been validated against British Gas balloon experiments (2) and the data of the Leeds combustion group (Abdel-Gayed et al (11)). The development of overpressures outside the module, such as caused by the combustion of unburnt gas vented into the atmosphere, are treated by a separate external combustion model. This sub-model is partly based upon an experimental study performed by British Gas (6) in which oxygen enriched

mixtures were employed to explore the effect of scale on the dynamics and combustion rates of the unburnt gas expelled from the explosion chamber.

CLICHE is being validated against data from explosions in a wide range of geometries and scales. To date, only homogeneous mixtures of fuel gas and air have been considered. Confined explosions in empty cuboidal vessels have been studied extensively by British Gas (Harris (12)) and provide pressure recordings and film of the flame for a range of vessel sizes and dimensions. These data provide a validation of the scale dependency of the laminar combustion model and the externally generated overpressures. Data on the flame acceleration induced by idealised equi-spaced obstacle arrays in cylindrical geometry are provided by multi-sponsored test programmes conducted both by the TNO Laboratories (Van Wingerden (13)) and the Chr. Michelsen Institute (CMI) (Björkhaug (14)). A preliminary validation against British Gas experiments studying representative offshore module geometries is also presented. Finally CLICHE predictions are compared against those of the CMI FLACS numerical model for some scenarios in Module C of the Piper Alpha platform considered during the inquiry (Bakke and Storvik (15)).

## THEORY

### Governing Equations and Numerical Solution

In general, the behaviour of the gas in an explosion is described by partial differential equations representing conservation of mass, energy and momentum which can be solved using finite difference techniques (8) but which require extensive computing resources. Ordinary differential equations, which are very much simpler to solve, are used in CLICHE. Similar approximations are made in CLICHE as in the classical single chamber confined explosion models ((9), (10)). These are applied to a volume with a single vent to atmosphere and are valid provided there are no significant spatial gradients of pressure within the volume. These approximations will, however, be invalid in many offshore geometries in which whole sides of modules can be open to the atmosphere or which contain many obstacles. CLICHE maintains the validity of the approximations by representing each module as a sequence of connected chambers. The simplified equations used in CLICHE are derived from the more complex equations by applying the conservation laws to the unburnt and burnt gas volumes in each chamber assuming that the pressure, density and gas properties are spatially uniform, and in addition that any momentum changes occur only at the perimeter of those volumes. This latter assumption removes the ability to predict the details of gas motion inside the volume except for the bulk mean flow velocity. The model, therefore, is unable to directly predict flame distortion, which results from the interaction of the flame with the flow field. Consequently, the flame shape has to be prescribed empirically as a function of the geometry and volume of burnt gas it encloses.

The equations describing each CLICHE chamber are given below including conservation equations of mass ( $M_u$ ;  $M_b$ ) and internal energy ( $M_u.C_u.T$ ;  $M_b.C_b.T$ ). In order to simplify the notation it has been assumed that the burning velocity ( $S$ ) is constant over the whole flame area ( $A$ ) and the calorific value ( $\Delta Q$ ) and specific heats ( $C_u$ ;  $C_b$ ) of the gas are constant. The chambers are connected to one another through the incoming ( $F_{in}$ ) and outgoing ( $F_{out}$ ) boundary fluxes of mass for both unburnt ( $F_{in}(p_u)$ ;  $F_{out}(p_u)$ ) and burnt gases ( $F_{in}(p_b)$ ;  $F_{out}(p_b)$ ). Since the specific internal energy ( $e$ ) differs between chambers there are also fluxes of internal energy ( $F(\rho \Delta e)$ ) caused by the differences in internal energy ( $\Delta e$ ) between chambers.



$$\frac{dM}{dt^u} + F_{out}(\rho_u) - F_{in}(\rho_u) + \rho_{uF} \cdot A_F \cdot S_u = 0 \quad (1)$$

$$\frac{dM}{dt^b} + F_{out}(\rho_b) - F_{in}(\rho_b) - \rho_{uF} \cdot A_F \cdot S_u = 0 \quad (2)$$

$$M_u \cdot C_{vu} \cdot \frac{dT}{dt^u} - F_{in}(\rho_u \Delta e_u) - A/W_u \cdot T_u \cdot \frac{dM}{dt^u} + P_F \cdot \frac{dV}{dt^u} = 0 \quad (3)$$

$$M_b \cdot C_{vb} \cdot \frac{dT}{dt^b} - F_{in}(\rho_b \Delta e_b) - \rho_{uF} \cdot \Delta Q \cdot A_F \cdot S_u - R/W_b \cdot T_b \cdot \frac{dM}{dt^b} + P_F \cdot \frac{dV}{dt^b} = 0 \quad (4)$$

The equation set for each chamber is completed by the constraint that the unburnt and burnt volumes must total to the chamber volume ( $V_T$ )

$$V_u + V_b = V_T \quad (5)$$

and by the ideal gas equations of state for unburnt and burnt volumes

$$R/W_u \cdot T_u \cdot M_u = P_F \cdot V_u ; \quad R/W_b \cdot T_b \cdot M_b = P_F \cdot V_b \quad (6)$$

It remains to describe the equations governing mass flux between the chambers, which for the simplest case of steady subsonic flow through a vent (Bird et al (16)) is given by the classical orifice equation, in terms of the upstream (1) and downstream (2) conditions

$$F(\rho) = A_2 \cdot [\rho_1/P_1]^{1/2} \cdot P_1 \cdot \left[ \frac{2\gamma}{\gamma-1} \cdot \frac{[1 - (P_1/P_2)^{(1-\gamma)/\gamma}]}{[(P_1/P_2)^{2/\gamma} - (A_2/A_1)^2]} \right]^{1/2} \quad (7)$$

where  $A_2$  and  $A_1$  are the area cross-sections of the approach flow to the orifice and the narrowest part of the vena contracta respectively.  $A_1$  ( $=C_v \cdot A_v$ ) is related to the vent area ( $A_v$ ) by a contraction coefficient ( $C_v$ ) which varies with the ratio  $A_2/A_1$ . This equation has a natural generalisation when the flow velocities through orifice become sonic and also, by appropriate selection of the contraction coefficient, can take account of the drag offered by obstacles using conventional 'rod bundle' correlations (16). The argument used to derive the above equation can also be applied when the mass flux is varying with time to obtain additional terms which arise due to the inertia of the gas and which give rise to additional pressure differentials. The equation set describing all chambers forms a system of coupled ordinary differential equations which are solved numerically in CLICHE using a general linear multistep algorithm (Oliver (17)).

The unburnt and burnt gas properties are calculated automatically by CLICHE from input definitions of the species in the fuel and oxidant gases. The properties, which are based upon the JANAF data (18), are based upon chemical equilibrium species for the burnt gas, which are calculated during the CLICHE simulation. These take account of temperature and pressure dependence. The potentially large computational overheads of the equilibrium calculation have been avoided by using a highly efficient numerical implementation (Erickson and Prabhu (19)).

### Combustion Model

In order to cater for general geometries, CLICHE has been interfaced with a detailed geometrical database of the module and plant. Fig. 1 shows a wireframe perspective of the obstacle geometry being used in the representative offshore experiments currently being performed by British Gas. Many of the bodies are pipes, but have been shown with square cross-section to speed up the visualisation software. CLICHE then processes the database to determine all of the parameters required for input to the combustion model. In particular, the analysis provides the variation with flame radius of the obstacle blockage as seen by the flame (Fig. 2). The combustion model is used to calculate the mass burning rate of the flame, which is given locally by the product of the flame area and the burning velocity. This is one of the most important parameters in the model since it directly controls the rate of flame acceleration. It therefore needs to describe the changing flame geometry, the obstacle induced drag and turbulence parameters.

**Flame Area.** Classically, the flame area is prescribed by an analytic expression ((9),(10)) which, even with the simplifying assumption that the flame curvature is spherical, limits the geometries and ignition positions that can be modelled. CLICHE, however, uses a numerically generated flame area, which enables the model to simulate ignition from any position within a cuboidal volume. The flame in its early stages of growth, following ignition, is assumed to take a spherical shape. Global distortion effects, such as the elongation of the flame towards a vent (Cooper (20)) or in a module with a long duct-like geometry, are treated by suitable empirical flame distortion correlations. When the flame interacts with obstacles it will also develop folds (Fig. 3) which grow as the flame passes the obstacles, and in which the burning rates are locally higher because of the turbulence generated in the obstacle wakes. The simulation results presented in this paper are all based upon a model which calculates the rate of growth of the flame folds from the known mean velocity of unburnt gas past the obstacles, and simulates the coalescence and eventual disappearance of the flame folds by assuming that they approach one another at twice the burning velocity (Fig. 3).

**Burning Velocity.** The local burning velocity is assigned to the maximum of the laminar and turbulent burning velocities, calculated from the known flame radius, root mean square (rms) turbulence velocity and turbulence integral length scale. If ignition occurs in a quiescent mixture the burning velocity is initially laminar, until the flame interacts with obstacles, when those parts of the flame downstream of the obstacles become turbulent. The turbulence parameters are based upon the mean flow velocities and the characteristics of the wake turbulence shed by the obstacles (Tennekes and Lumley (21)). The model also caters for the situation when there is some residual turbulence at the time of ignition as would be the case if water sprays were operating or possibly due to the fuel release itself. The turbulence kinetic energy in these cases are deduced from the kinetic energy imparted to the flammable atmosphere by the spray or jet, and the turbulence length scales are determined from the sizes of obstacles and/or the dimensions of the confining region.

The laminar burning velocity is based upon empirical correlations of the flame speed and the flame radius which were determined from balloon experiments conducted by the Midlands Research Station at the Pauld Test site (2). These experiments, which were performed for a range of hydrocarbon / air mixtures, demonstrate how the averaged burning velocity increases with flame radius, due to wrinkling of the flame's surface. This is caused by a natural

flame instability (Williams (22), Lind and Whitson (23) which must be taken into account if a model is to predict correctly the scale dependence of explosions ignited in a quiescent gas (3).

The turbulent burning velocity is based upon a Kolmogorov, Petrovsky and Piskounov (KPP) analysis (24) of the theoretical combustion model due to Bray (25) which has been calibrated against the extensive turbulent burning velocity measurements made by the Leeds University combustion group (11). Examples of the agreement achieved for methane / air mixtures over a range of stoichiometries is given in Fig. 4. This model, which is based upon the assumption that the turbulent flame is an ensemble of laminar flamelets, takes account of the quenching of the flamelets by the turbulence strain field. It is this process which limits the increase in turbulent burning velocity caused by increases in the rms velocity fluctuations. For a given rms velocity, more quenching occurs as the turbulence integral length scale gets smaller. Modelling these scale effects is a crucial requirement of the model, in order to make predictions of full-scale scenarios, since reduced scale experiments are the only source of data with which to validate the model.

#### External Explosion Model

Combustion in a region of confinement causes the unburnt gas ahead of the flame to be expelled through the perimeter vents. Since the exit velocity is changing continuously, typically increasing rapidly as the mass burning rate grows, the external flow takes the form of a transient jet characterised by a 'stalk', which is like that of a steady jet, at the head of which there is a mushroom-like ball of gas (6). The head will be turbulent since it contains the gas convected from the shear layers on the perimeter of the stalk. At a later stage in the explosion, combustion products are ejected from the vent (20) which propagate along the jet and can give rise to an external explosion. The explosion causes a pressure wave which can provide an external blast source in itself (Harrison and Eyre (26)) but, on reaching the vent, also has the effect of restricting the gas from being vented. This can cause the overpressures in the confined region to reach a much higher level than had the external explosion not occurred. The complex jet dynamics and external combustion involved in this type of explosion were studied systematically in a range of experiments conducted by British Gas (6). The overpressures generated in the external combustion were found to depend upon the magnitude and history of the jet exit velocity, the composition of the flammable vapour and whether the external atmosphere comprised of air or flammable mixture. The magnitude of the pressure wave arriving at the vent also depended upon how far away from the vent the external explosion occurred.

The model of the transient jet is represented by a sequence of impulsively started jets. Each propagates at that velocity relative to the atmosphere ahead of them which ensures that the stagnation pressures of the gas being displaced by the head and that being vented are in equilibrium. This calculation provides the propagation speed of the jet head and hence its position. By totalling the flux of gas arriving at the jet head through time, the volume of the jet head at the time of its ignition by the vented product gas is also calculated. The burning velocities in the turbulent head are determined from empirical correlations, derived from the experimental programme (6). In order to study the effects of gas exit velocity and fuel reactivity systematically, the rig was specially constructed to allow turbulence to be induced in the confined explosion chamber. By varying the turbulence level, the vent velocity history could be varied widely, whilst

maintaining the same flammable mixture. An array of pressure transducers were mounted outside the vent to determine the position and peak overpressure at the explosion centre; the latter of which was correlated to the velocities in the head at ignition (6). In order to compensate for scale effects, mixtures of the fuel gas and oxygen enriched air were used to provide a tentative extrapolation to experimental scales eight times larger than the 1.8m x 0.6m x 0.6m chamber employed. The external explosion, and the propagation of the pressure wave towards the vent, are described approximately by an acoustic model (Strehlow (27), Catlin (28)) for peak overpressures below 300 mbar. This assumes a spherical flame and the empirically derived peak overpressure ( $\Delta P_{max}$ ) and flame speed ( $S_f$ ). The overpressure ( $\Delta P$ ) at a radial distance  $r$  from the explosion centre, therefore, increases with time ( $t$ ) according to the formula below, where  $a_o$  is the speed of sound in ambient air.

$$\Delta P = \Delta P_{max} \cdot S_f / (a_o - S_f) \cdot (a_o t - r) / r ; a_o t > r$$

This overpressure returns to ambient upon arrival of the rarefaction wave caused by the deceleration of the flame when it has burnt through the turbulent gas in the head. For higher overpressures, different assumptions are required since the peak overpressure no longer decays inversely with distance (27).

#### VALIDATION

##### Confined Explosions in a Single Empty Vessel

British Gas has been engaged in a programme of work related to explosions in buildings for many years (12) and has constructed a range of cuboidal explosion chambers at their Fauld Test Site. Those chambers which provided the data reported here vary in size between a 1.7m x 1.2m x 1.2m cuboid and a 3m cube. In the cases simulated, the chamber was filled with a homogeneous mixture of natural gas (94% CH<sub>4</sub>:6% C<sub>2</sub>H<sub>6</sub>) and air of stoichiometric concentration, and the ignition position was central to the volume. All chambers had a single vent whose size and cover strength were varied. A range of failure pressures were studied, the lowest being a polythene vent cover, with higher strengths achieved by using different types of wooden boarding. The data that are available for validation are more extensive than reported here, and include experiments in chambers with duct-like geometries, non-homogeneous mixtures and a variety of fuel gases and ignition positions.

Fig. 5 shows typical agreement, for what shall be referred to as the P1 and P2 peaks (20), in the early stages of an explosion in the smaller vessel. These peaks correspond respectively to the failure of the vent, whose failure pressure is 21 mbar in this test, and the pressure surge that arises in the chamber due to an external explosion. The intermediate peak ( $P_{BV}$ ) corresponds to the onset of burnt gas venting, which causes a sharp fall in the overpressure (20). The model has been found to correlate the experimentally measured variation in the P2 peak with a wide range of vent coefficients (K) and vent failure pressures (Figs. 6 and 7). Note that the vent coefficient (K) is defined as the ratio  $V^{2/3}/A$  where V is the chamber volume and A the vent area. CLICHE is also able to predict the significantly higher overpressures measured in a larger 27 m<sup>3</sup> cube, which demonstrates the validity of the assumptions on scale dependence used in the combustion model. Fig. 8 gives a comparison for the entire explosion showing the agreement with P1, P2 and P3 peaks. The P3 peak corresponds to the maximum burning rate, which occurs close to the time when the flame area is



at its maximum (20). In this particular experiment the transducer was affected by the heat of the combustion products which led to an undermeasurement of the peak overpressure. It should be noted that CLICHE does not include a model for the oscillatory (P4) combustion peak, discussed in (20), since it is considered to be irrelevant to the majority of realistic explosion scenarios. This peak has been demonstrated to be caused by a positive feedback mechanism between acoustic oscillations and the flame, when the chamber is almost completely full of combustion products. Anything which can cause disruption of the acoustic resonances, whether by absorbent material or by the additional reflecting surfaces provided by obstacles, will prevent this final surge in internal pressure.

#### Confined Explosions With Repeated Obstacle Arrays in Cylindrical Geometry

There are a wide range of experiments that have been conducted under multi-sponsored funding both by the TNO laboratories (13) and Chr. Michelsen Institute (14) in which flame acceleration has been studied in repeated obstacle arrays in an idealised cylindrical geometry. This geometry can be accurately represented in the CLICHE model. The size, shape and relative separation of obstacles vary between the experiments, and the experimental scale also varies widely between the 1.2 m radius semicircular rig used by TNO (13) and the 1 m and 10 m radius sectors used by CMI (14). The validation calculations described here are against the TNO pressure/time data. However, equally satisfactory agreement with the quoted peak overpressures from the CMI 10 m rig was also achieved, thus indicating the validity of the scale dependency of the turbulent combustion model.

In the TNO experiments, the cylindrical obstacles are arranged in concentric circles (Fig. 3) about the ignition point, and therefore the region between each obstacle array can be modelled as a separate CLICHE chamber. The separation distance between the obstacles was the same in each array, hence providing the same blockage, and the arrays were equally spaced in the radial direction. In the experiments simulated, the 8 arrays of 0.08 m diameter obstacles had 50% blockage and were confined by a solid roof. Each array was separated by a distance of 3 obstacle diameters. Photographs taken through the transparent roof showed (13) that folds formed on the flame as it passed each obstacle array. These folds later coalesced, as is assumed in the computer model (Fig. 3). The measured pressure pulses indicate that as the flame passed each obstacle array there was an increase in the mass burning rate. CLICHE was able to predict these pulses (Fig. 9). In the simulation the pressure differentials between chambers increased, which simultaneously increased the flow and turbulence velocities. This, together with the additional flame area caused by the folds, caused large increases in the burning rates downstream of each obstacle array. The close agreement between the predicted pressures and the measurements in the experiments with stoichiometric methane and propane / air vapour are shown in Fig. 9. The peak, duration and even the character of the overpressure pulses are closely reproduced, but the times from ignition were underpredicted. This discrepancy is probably not important, since it only represents a small error between the predicted and experimental laminar burning velocities. This is because the largest part of the time delay between ignition and the peak overpressure is caused by the initial slow laminar flame. After the flame's interaction with the first obstacle array, when the combustion becomes turbulent, the flame speeds rapidly increase. Although ethylene / air mixtures were used in the majority of TNO experiments, the methane and propane experiments were considered the best for validation purposes since these fuel gases are the most relevant to offshore applications.

#### Realistic Offshore Geometries

The scope for validating theoretical models is presently limited by the experimental data available. 1/5th-scale experiments in idealised compression and separator geometries have been conducted by CMI but only peak overpressures have been published to date (Hjertager (29)). It was therefore considered equally constructive to compare the predictions of CLICHE with some of the simulations performed for the Piper Alpha inquiry by CMI using the FLACS code (15). Because of the lack of data, British Gas have embarked upon an experimental programme to study more representative offshore geometries, including representations of the detailed pipework and supports found in typical offshore modules. A comparison between CLICHE and some preliminary data are also given below.

Fig. 10 shows an overhead view of the Piper Alpha module, which was idealised in the CLICHE simulations by 8 chambers. The 8 corresponding pressure monitoring positions (C1-8) along the centre line of the module are also shown together with the eight edge positions (P1-8) used in the FLACS simulations. The ignition position was taken on the centre line, just inside the eastern end of the module, where the flammable vapour cloud was located. The roof and floor of the module were taken to be solid, but the north and south walls were modelled to have 20% porosity as an approximate description of the failure of the boundary which was assumed to occur at a low overpressure. The CLICHE simulations were performed assuming a stoichiometric methane/air mixture. Although the FLACS calculations assumed an 88% methane/ 12% ethane mixture this was not considered to have a significantly different burning rate from methane because the overpressures did not reach sufficiently high levels for the ethane chemistry to become important. Two FLACS calculations were reported (15) for the cases when the module was 30% and 50% filled with gas. One CLICHE simulation, which assumed the module completely full of gas was performed. The pressure/time variation at the 8 positions is given in Fig. 11, which clearly shows the peak overpressures to increase toward the western end of the module. The general question of how the peak overpressure may vary with the fraction of the module filled with flammable gas was answered by modelling the movement of the flammable boundary. In fact, the boundaries of a range of differently sized vapour clouds were tracked simultaneously. The peak overpressure for each cloud size was assumed to correspond to when the flame reached the flammable boundary, and hence when the flame extinguished. The peak overpressure in each of the 8 chambers at the time the flame extinguished is given in Fig. 12 which is compared to the average of the values predicted by FLACS on the north and southern sides. Clearly the two models are in reasonable close agreement.

The geometry of the rig being used in the British Gas representative offshore experiments can be inferred from Fig. 1, which shows the layout of pipework which is enclosed by a perimeter cuboid 9m x 4m x 2.1m. The roof, floor, west and north sides of the rig are closed by solid steel walls which are not shown on Fig. 1. The east and south sides are open to the atmosphere. The pipework is roughly bounded by two cuboids running east to west the northern most region being the taller (1.75 m), the southern region (1.25 m) leaving an 0.85 m empty gap between the obstacles and the roof. The experiment simulated with CLICHE had an initially quiescent stoichiometric mixture of natural gas (96% CH<sub>4</sub>:4% C<sub>2</sub>H<sub>6</sub>) and air, which was ignited at a point central to the closed north wall of the rig. Although the west side of the rig was closed, the flame was seen initially to develop symmetrically in the eastern and western directions, and the peak overpressures measured within the framework were evenly distributed. Fig. 13 shows the similarity

in pressure profiles at two internal pressure transducers, roughly 1.5 and 3m from the ignition point. The volume was broken down into 8 chambers in the CLICHE simulation, each chamber bounded by a spherical surface separated by 0.5m. The predicted overpressure/time profiles at the centres of the 8 chambers (Fig. 13) show a very similar pressure development in the first 5 chambers, in agreement with the experiment. The predicted peak overpressure is approximately 50 mbar less than that measured, but the predicted duration is almost twice as large. This result indicates some limitations in the modelling parameters currently being used in CLICHE which are apparently causing an underprediction in the flame speed. However, it is for these detailed pipe geometries with comparatively low blockage (Fig. 2) that CLICHE has been least validated and for which the model is currently being improved.

#### CONCLUSIONS

The CLICHE explosion model is currently being developed by British Gas to provide a practicable and generally applicable model for use by engineers for making explosion hazard assessments of offshore platforms. The basic theory of CLICHE has been described, indicating why it is equally applicable to explosions with and without perimeter confinement, and to geometries typical of offshore modules which contain large amounts of pipework and plant. Unlike many of the simpler explosion models, which rely heavily upon empirical correlations based on experimental data, CLICHE is fundamentally based, with turbulence and combustion submodels which take account of the important scale dependent processes. The interaction between the flame and the flow field is taken into account in CLICHE by using flame distortion correlations. The external explosion model is partly empirical with scale effects being compensated for in the experiments by using oxygen-enriched mixtures. CLICHE predictions have been compared against a variety of different experiments, and also against the predictions of the CMI explosion model FLACS. CLICHE provides very good agreement with the confined explosion data of British Gas for explosion chambers up to 27m<sup>3</sup> in volume, and also against the data of TNO and CMI for cylindrical flame acceleration through repeated obstacle arrays in rigs between 1 and 10m radii. These results demonstrate the ability of the model to predict scale effects. The comparison study between CLICHE and British Gas data for representative offshore geometries is presently at a preliminary stage, but the results are in encouraging agreement. Similarly, reasonably close agreement was obtained with the complex numerical code FLACS, for explosion scenarios in Module C of the Piper Alpha platform as reported to the Piper Alpha Inquiry.

#### ACKNOWLEDGEMENT

This paper is published by permission of British Gas plc.

#### NOMENCLATURE

$a_0$	= speed of sound in ambient air	(m/s)
A	= area	(m <sup>2</sup> )
$A_F$	= flame area	(m <sup>2</sup> )
$A_v$	= explosion chamber vent area	(m <sup>2</sup> )
$C_D$	= contraction coefficient	

$C_v$	= specific heat at constant volume	(J/(kg K))
F	= flux of conserved quantity	
M	= total mass of gas	(kg)
P	= pressure	(N/m <sup>2</sup> )
r	= radial distance from external explosion centre	(m)
R	= Universal gas constant	(J/(kmol K))
$S_u$	= burning velocity	(m/s)
$S_F$	= flame speed	(m/s)
t	= time	(s)
T	= temperature	(K)
$U_p$	= particle velocity	(m/s)
V	= volume	(m <sup>3</sup> )
$V_T$	= total chamber volume	(m <sup>3</sup> )
W	= molecular weight	(kg/kmol)
$\rho$	= density	(kg/m <sup>3</sup> )
$\gamma$	= ratio of specific heats	
$\Delta P$	= overpressure relative to ambient	(N/m <sup>2</sup> )
$\Delta P_{max}$	= peak overpressure at external explosion centre	(N/m <sup>2</sup> )
$\Delta Q$	= calorific value of flammable gas	(J/kg)

#### SUBSCRIPTS

b	burnt state	u	unburnt state	F	state at flame
1	upstream state	2	downstream state		

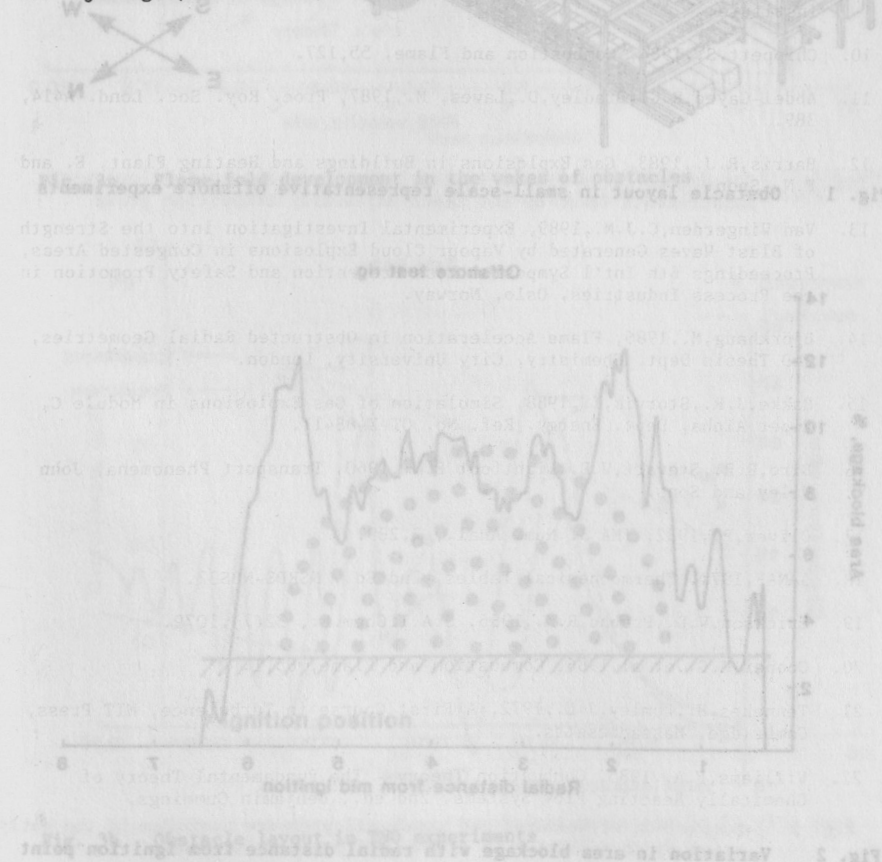
#### REFERENCES

- Chamberlain, G.A., 1989, The Nature and Mitigation of Vapour Cloud Explosions, The Cullen Inquiry into the Piper Alpha Incident.
- Harris, R.J., Wickens, M.J., 1989, Understanding Vapour Cloud Explosions - An Experimental Study; 55th Autumn Meeting of the Institution of Gas Engineers.
- Van Wingerden, C.J.M., 1989, Chemical Engineering Research and Design 67, 339.
- Catlin, C.A., Johnson, D.M., 1990, An Experimental Investigation into Scaling Techniques for Studying the Flame Acceleration Phase of an Explosion (Submitted to Combustion and Flame).



5. Taylor, P.H., 1988, The Scaling of Vapour Cloud Explosions: A Fractal Model for Size and Fuel Type, Poster paper at 22nd Symposium (Int'l) on Combustion, Seattle.
6. Catlin, C.A., 1990, Scale Effects on the External Combustion Caused by Venting of a Confined Explosion, (Due to appear in Combustion and Flame).
7. British Gas Midlands Research Station, 1990, Review of the Applicability of Predictive Methods to Gas Explosions in Offshore Modules, HMSO Report No. OTH 89 312.
8. Bakke, J.R., 1986, Numerical Simulation of Gas Explosions in Two-Dimensional Geometries, PhD Thesis Faculty of Mathematics and Natural Sciences, University of Bergen.
9. Fairweather, M., Vasey, M.W., 1982, A Mathematical Model for the Prediction of Overpressures Generated in Totally Confined and Vented Explosions, Proceedings 19th Symposium (Int'l) on Combustion, The Combustion Institute.
10. Chippett, S., 1984, Combustion and Flame, 55, 127.
11. Abdel-Gayed, R.G., Bradley, D., Lawes, M., 1987, Proc. Roy. Soc. Lond. A414, 389.
12. Harris, R.J., 1983, Gas Explosions in Buildings and Heating Plant, E. and F.N. Spon.
13. Van Wingerden, C.J.M., 1989, Experimental Investigation into the Strength of Blast Waves Generated by Vapour Cloud Explosions in Congested Areas, Proceedings 6th Int'l Symposium Loss Prevention and Safety Promotion in the Process Industries, Oslo, Norway.
14. Björkhaug, M., 1986, Flame Acceleration in Obstructed Radial Geometries, PhD Thesis Dept. Chemistry, City University, London.
15. Bakke, J.R., Storvik, I., 1988, Simulation of Gas Explosions in Module C, Piper Alpha, Dept. Energy. Ref. No. OT-X-88411.
16. Bird, R.B., Stewart, W.E., Lightfoot, E.N., 1960, Transport Phenomena, John Wiley and Sons.
17. Oliver, P., 1982, IMA J. Num. Anal., 2, 289.
18. JANAF, 1971, Thermochemical Tables, 2nd Ed., NSRDS-NBS37.
19. Erickson, W.D., Prabhu, R.K., 1986, J.A.I.Chem.E., 32(7), 1079.
20. Cooper, M.G., et al, 1986, Combustion and Flame, 65, 1.
21. Tennekes, H., Lumley, J.L., 1972, A First Course in Turbulence, MIT Press, Cambridge, Massachusetts.
22. Williams, F.A., 1985, Combustion Theory - The Fundamental Theory of Chemically Reacting Flow Systems, 2nd ed., Benjamin Cummings.

23. Lind, C.D., Whitson, J., 1977, Explosion Hazards Associated with Spills of Large Quantities of Hazardous Materials. Phase II - Department of Transportation U.S. Coast Guard Report No. CG-D-85-79.
24. Kolmogorov, A., Petrovsky, I., Piskunov, N., 1937, Bull. MGU Moscow State University, USSR, Section A, 1(6).
25. Bray, K.N.C., 1987, Scales and Burning Rates in Premixed Turbulent Flames, 9th Australasian Fluid Mechanics Conference, Auckland, New Zealand.
26. Harrison, A.J., Eyre, J.A., 1987, Comb. Sci. Tech., 52, 91.
27. Strehlow, R.A. et al, 1979, Combustion and Flame, 35, 297.
28. Catlin, C.A., 1985, An Acoustic Model for Predicting Over-Pressure Caused by the Deflagration of a Ground Lying Vapour Cloud, IChemE Symp. Series No. 93.
29. Hjertager, B.H. et al., 1988, J. Loss Prev. Process Ind., 1, 197.



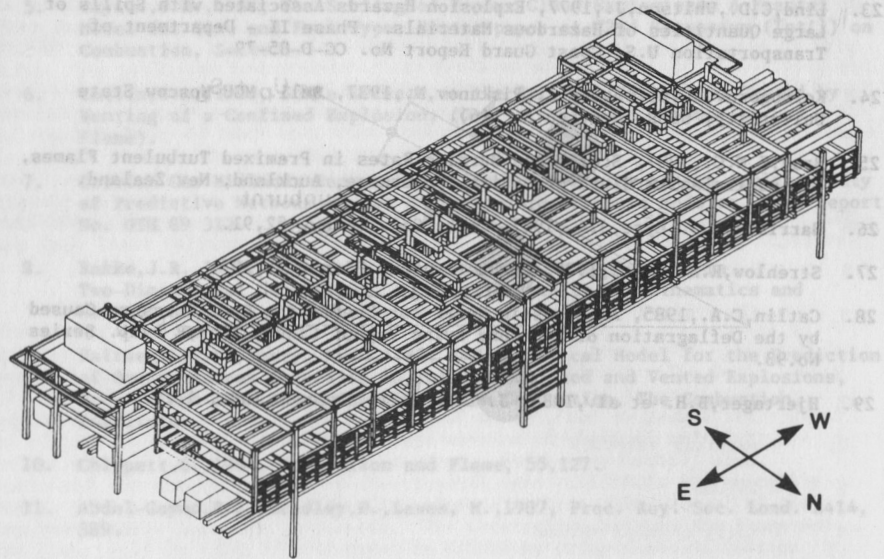


Fig. 1 Obstacle layout in small-scale representative offshore experiments

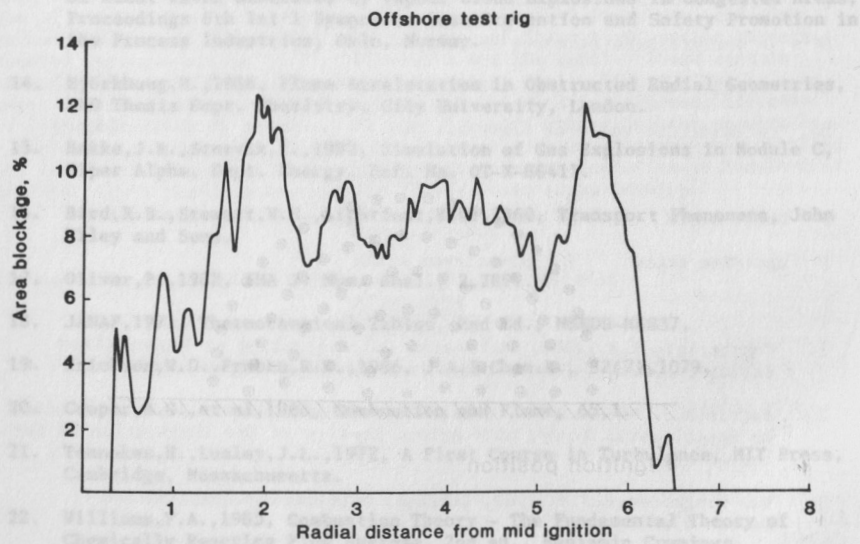


Fig. 2 Variation in area blockage with radial distance from ignition point

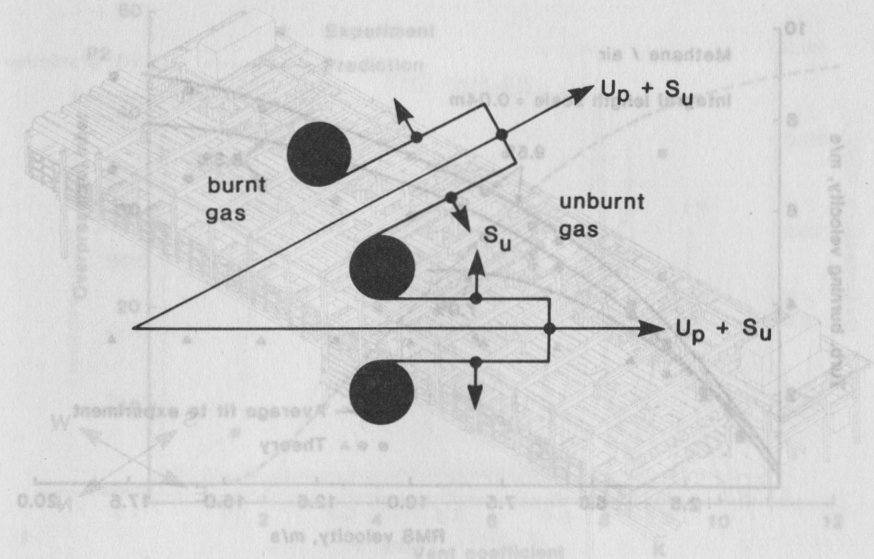


Fig. 3a Flame fold development in the wakes of obstacles

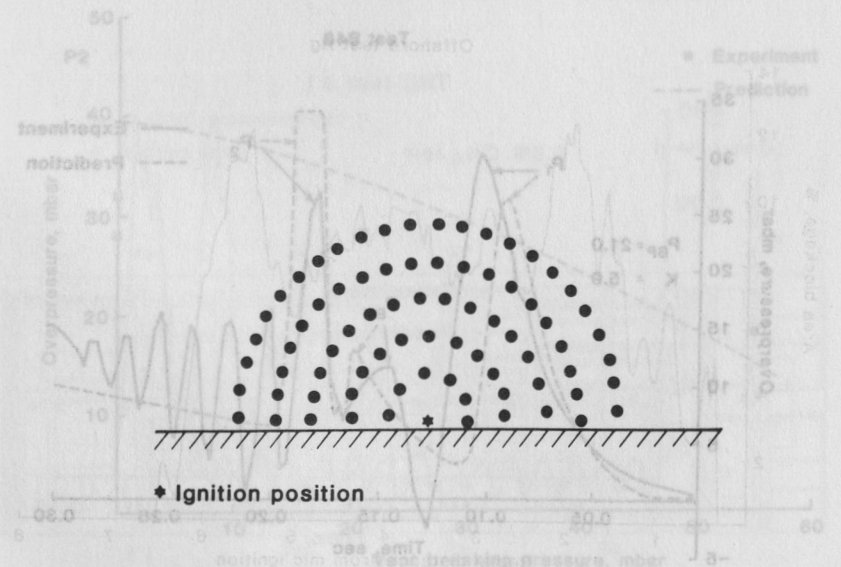


Fig. 3b Obstacle layout in TNO experiments



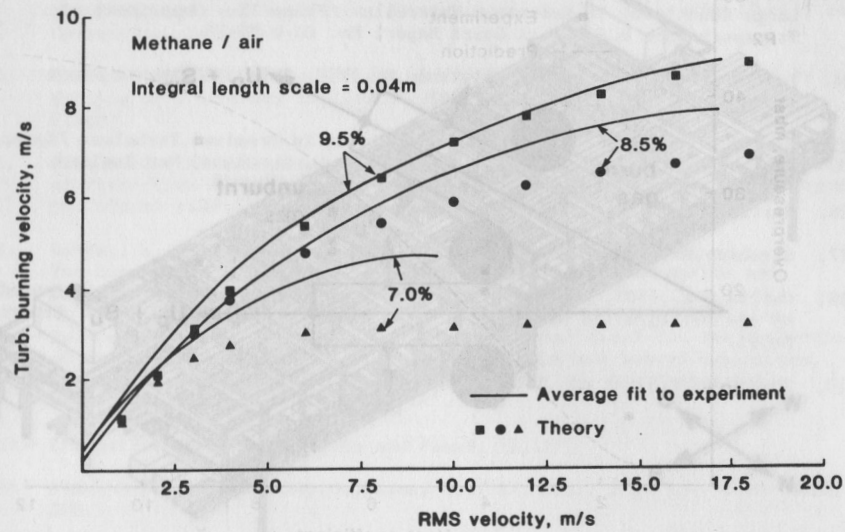


Fig. 4 Comparison of turbulent burning velocity model predictions with measurements taken by the Leeds University combustion group

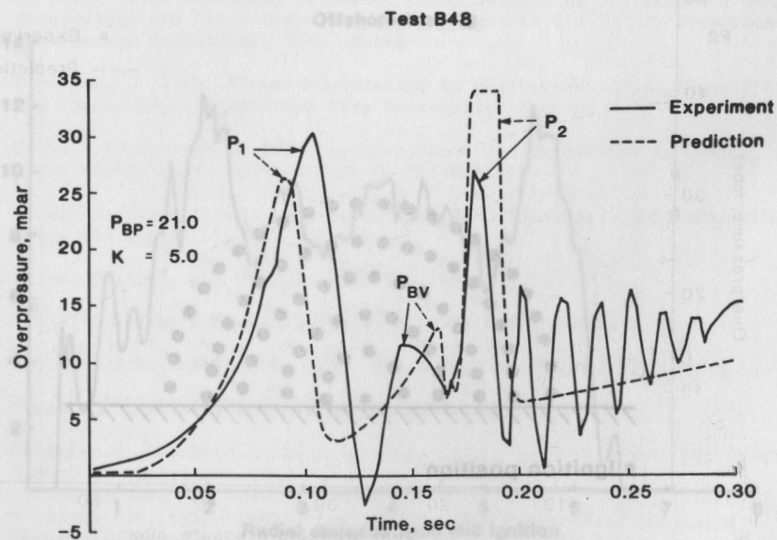


Fig. 5 Comparison of measured and predicted pressure profiles in the early stage of an explosion in a 1.7m x 1.2m x 1.2m chamber

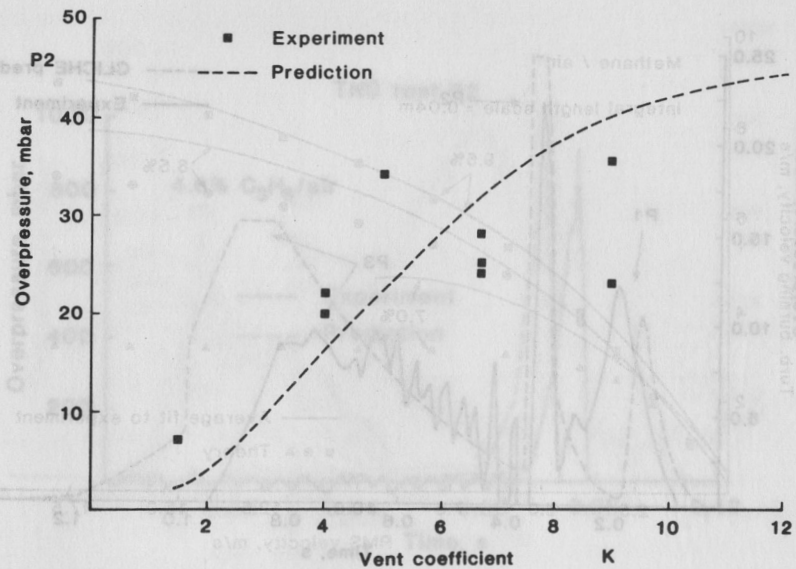


Fig. 6 Comparison of measured and predicted variation in P2 with the vent coefficient for a vent with nominally zero failure pressure

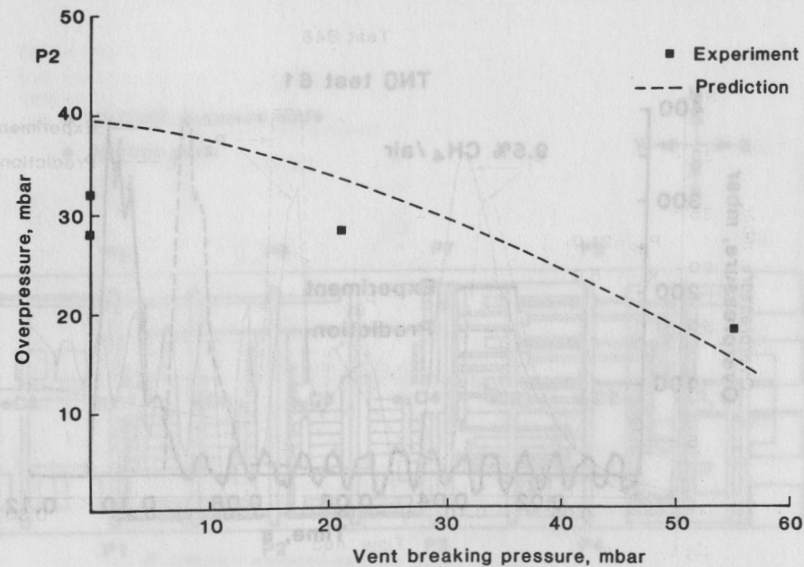


Fig. 7 Comparison of measured and predicted variation in P2 with vent failure pressure for a vent with coefficient K = 5

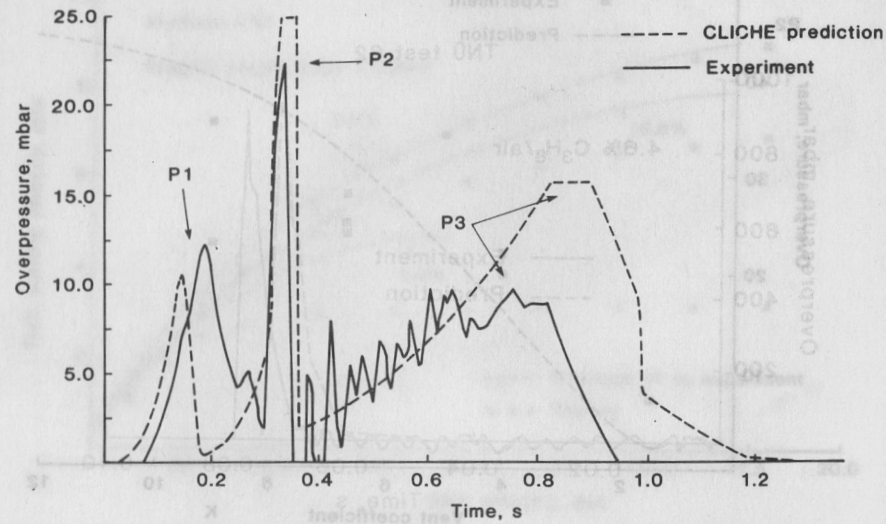


Fig. 8 Comparison of measured and predicted pressure profiles for an explosion in the 3m cubical chamber

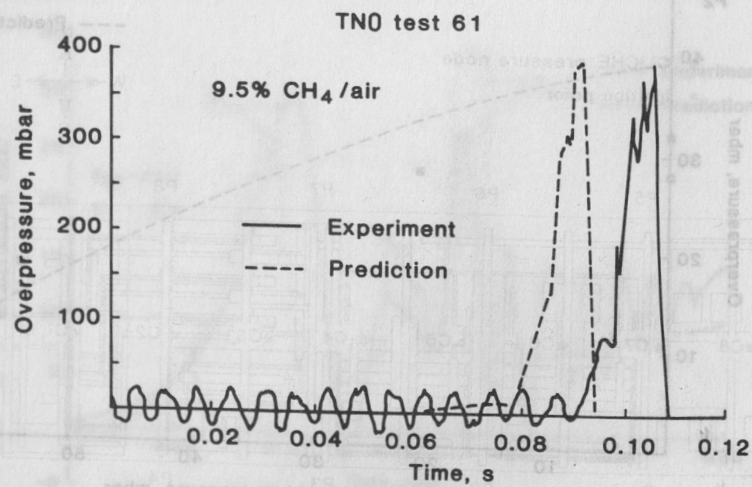


Fig. 9a Measured versus predicted overpressure for the TNO methane / air experiment

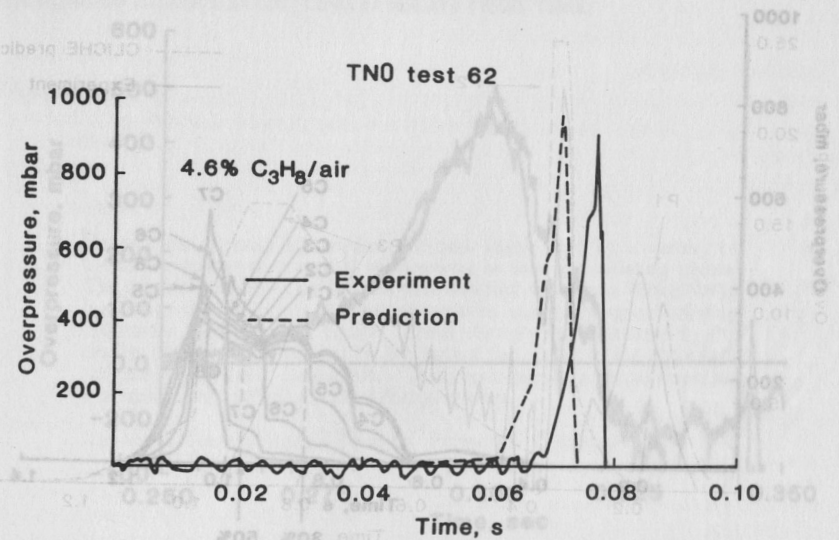


Fig. 9b Measured versus predicted overpressure for the TNO propane / air experiment

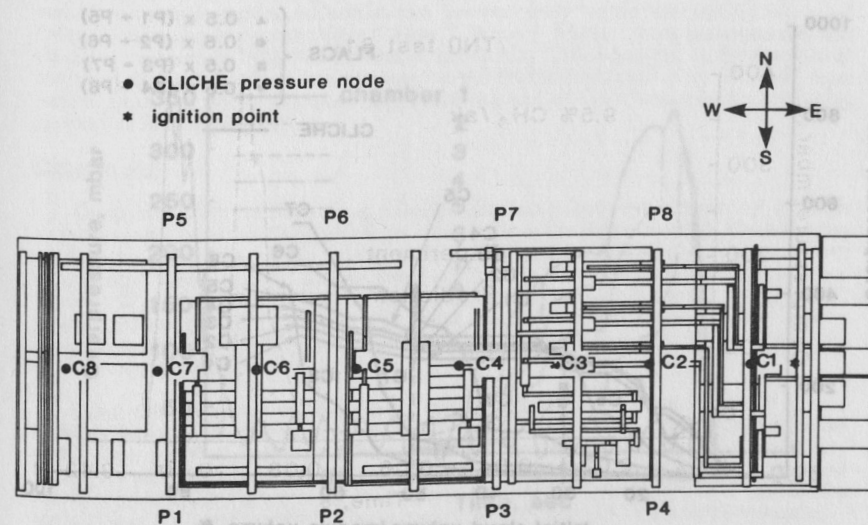


Fig. 10 Plan view of the Piper Alpha Module-C showing the pressure monitoring positions used in the CLICHE and FLACS simulations



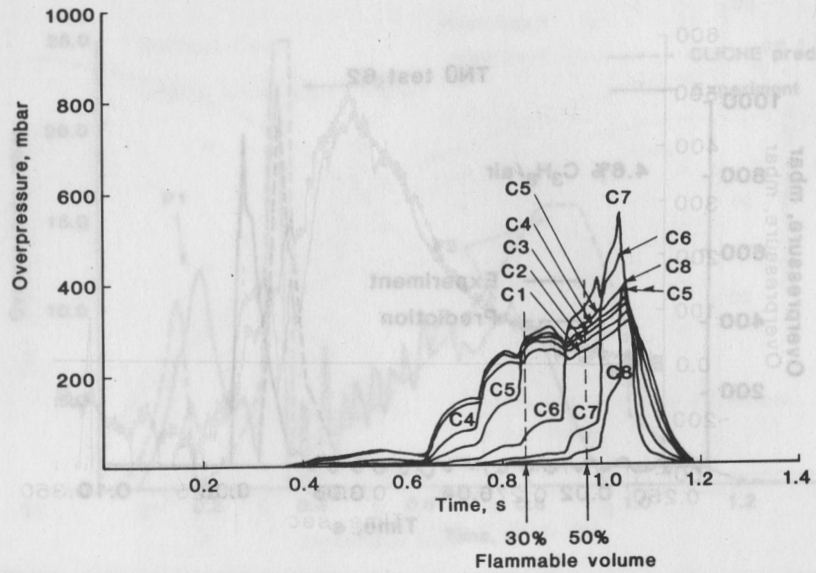


Fig. 11 Pressure/time at 8 monitoring positions in the CLICHE simulation assuming the module completely full of methane/air mixture

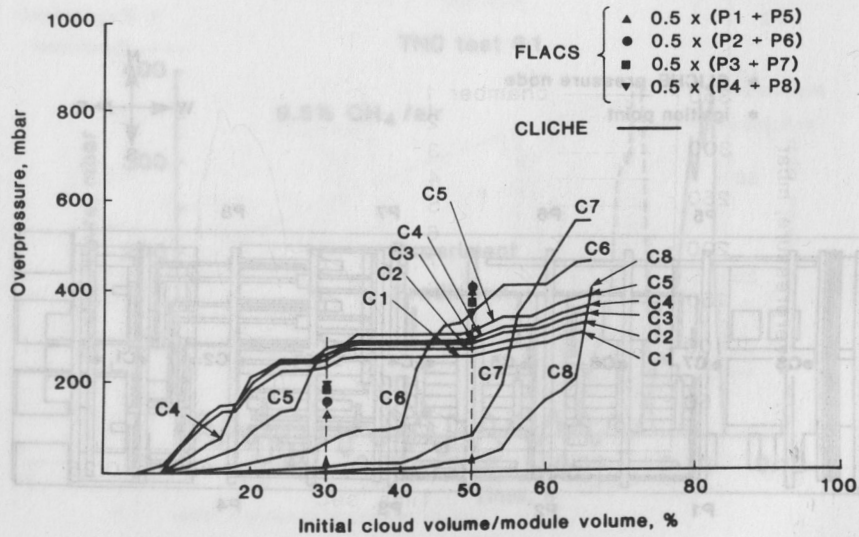


Fig. 12 Peak overpressures for different initial vapour cloud sizes predicted by CLICHE and FLACS models

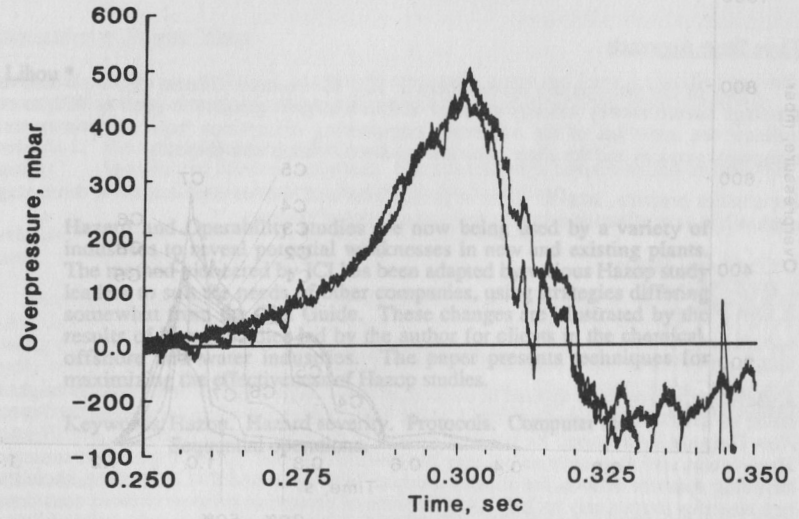


Fig. 13a Measured overpressures at two locations in the small-scale offshore experiment

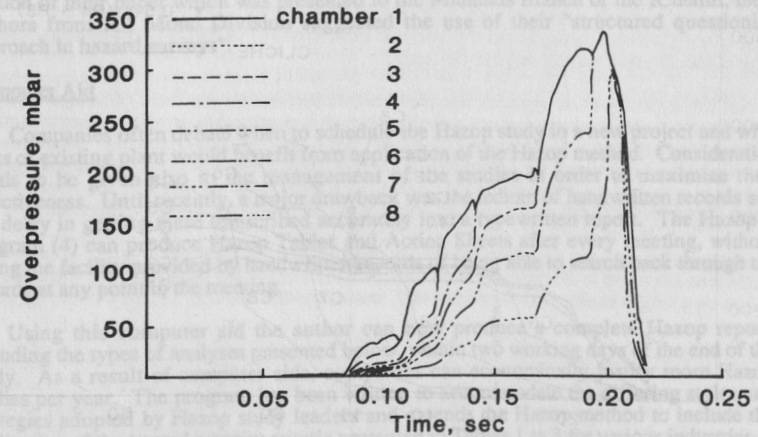


Fig. 13b Overpressures predicted by CLICHE for small-scale offshore experiment